Environment International 214 (2026) 110400

Contents lists available at ScienceDirect

Environment International

journal homepage: www.elsevier.com/locate/envint

Full length article

Investigating fish eye lenses as chemical archives of organic pollutant exposure

Rebekah Boreham [a,*], Philip White [b], Boyd A. McKew [a], Sara Leston [c,d], Andreia Freitas [e,f], Jonathan L. Barber [g], Michael Williamson [h,i], Adam Piper [h], Rosie Williams [h], Anna M. Sturrock [a]

[a] University of Essex, School of Life Sciences, Wivenhoe Park, the United Kingdom of Great Britain and Northern Ireland
[b] Marine and Freshwater Research Centre at the Atlantic Technological University, Galway, Ireland
[c] CFE – Centre for Functional Ecology, TERRA Associate Laboratory, Department of Life Sciences, University of Coimbra, Calçada Martim de Freitas, 3000-456 Coimbra, Portugal
[d] Pharmacy Faculty, Pólo das Ciências da Saúde, Azinhaga de Santa Comba, 3000-548 Coimbra, Portugal
[e] National Institute for Agricultural and Veterinary Research (INIAV), Rua dos Lágidos, Lugar da Madalena, 4485-655 Vila do Conde, Portugal
[f] REQUIMTE/LAQV, Faculty of Pharmacy, University of Porto 4050-313 Porto, Portugal
[g] Centre for Environment, Fisheries and Aquaculture Sciences, Lowestoft, the United Kingdom of Great Britain and Northern Ireland
[h] Institute of Zoology, Zoological Society of London, Regent's Park, London NW1 4RY, the United Kingdom of Great Britain and Northern Ireland
[i] Environment and Sustainability Institute, University of Exeter, Penryn Campus, Penryn, Cornwall TR10 9FE, the United Kingdom of Great Britain and Northern Ireland

ARTICLE INFO

Keywords:
GC–MS/MS
Archival Structures
PAHs
Biochronology
Ecotoxicology

ABSTRACT

To target pollution remediation efforts and predict pollutant impacts on fisheries and food security, new tools are needed to reconstruct lifetime exposure histories for endangered and commercially valuable fishes. However, current methods used to quantify chemical burden typically use soft tissues which lack temporal information and can miss pulse exposures. Fish eye lenses are proteinaceous structures that form metabolically inert layers (laminae) through life. Their isotopic chronologies are widely used to track lifetime habitat use and diet, but organic pollutants have not previously been quantified in this tissue for fish. Other metabolically inert archival tissues, such as otoliths, are also popular for isotopic life history reconstruction, but almost entirely comprise calcium carbonate with very low protein or lipid content compared with the eye lens, which we show here contain low but measurable levels of lipids, as much as 3.5% w/w in European eels, and so have a greater affinity to bind organic chemicals.

To reconstruct pollutant exposure events, a key first step is to show which, if any, chemicals bind to eye lenses. Hence, the present study developed methods to detect organic pollutants in the eye lenses of common dab (*Limanda limanda)* and European eel (*Anguilla anguilla)* using GC–MS/MS. For the first time, multiple polycyclic aromatic hydrocarbons were detected in lens tissue, with total concentrations positively correlated to those measured in paired liver samples. However, eye lenses generally contained fewer analytes, likely reflecting a lower bioaccumulation capacity compared with lipid-rich livers. More targeted analysis is needed to achieve lamina-level (chronological) resolution, and controlled exposure experiments to validate relationships with ambient concentrations and establish the underlying pathway(s). Nevertheless, eye lenses show potential as archives of historical organic pollutant exposure.

1. Introduction

Aquatic wildlife are particularly vulnerable to the effects of pollution as waterways act as a sink for countless types of contaminants discharged via run-off from landfill, waste-water treatment works (WWTP), urban and industrialised areas, and agriculture (Pal et al., 2010; Malaj et al., 2014; Benedetti, Giuliani and Regoli, 2015; Du Plessis, 2019). Deleterious effects in fish can range from altered behaviour (Jacquin et al., 2020; Olivares-Rubio and Arce, 2023), to endocrine disruption (Barra et al., 2021) to oxidative stress (Mustafa, Al-Rudainy and Salman,

* Corresponding author.
E-mail address: r.boreham@essex.ac.uk (R. Boreham).

https://doi.org/10.1016/j.envint.2026.110400
Received 31 October 2025; Received in revised form 29 May 2026; Accepted 1 July 2026
Available online 5 July 2026

2024). Such factors resulting from chronic exposure can lead to population decline (Hamilton et al., 2016). Additionally, increasing frequency of extreme weather events (Wang et al., 2022), together with changing land use and socio-economic/demographic developments (Whelan et al., 2022) is likely to intensify point source contamination and pulse exposure events. This contributes to increasing severity in mass mortality events in fish (Fey et al., 2015), with potential impacts for ecosystems and commercial fisheries (Neis et al., 2023).

To target efforts to protect aquatic habitats, there is an urgent need to monitor pollution levels through time and to understand their impact on biota. Additionally, being able to link a physiological outcome observed in a fish to an exposure event earlier in life could elucidate sub-lethal or carry-over effects of that contaminant (Johnson et al., 2020). The concept of the 'eco-exposome', which describes the totality of internal chemical exposure across an organism's lifetime, is also gaining popularity for its potential as a framework to more comprehensively understand the exposure and resulting health effects of chemical mixtures in the environment (Scholz et al., 2022). However, current standard methods to quantify chemical burden in fish tend to use soft tissues such as liver and muscle, which have relatively fast turnover rates, typically in the order of weeks to months (Madigan et al., 2012; Barton et al., 2019). Such tissues provide a reliable representation of recent exposures and an indication of human health risk among consumed species, however, they cannot resolve the timing of exposure and can thus miss historical or pulse exposures.

Metabolically inert tissues, such as eye lenses and otoliths, incorporate ions and compounds into their growth layers across the entire lifetime of the animal (Tzadik et al., 2017). Such archival structures can provide a permanent, chronological record of the fish's experience by incorporating markers such as elemental and stable isotope ratios, and endogenous hormones. These markers can reveal aspects of their physiology (Aerts et al., 2015; Charapata, Horstmann and Misarti, 2021; Charapata et al., 2022), diet (Bell-Tilcock et al., 2021; Sakamoto et al., 2023; Golikov et al., 2024) and ambient physicochemical conditions (Volk et al., 2000; Limburg et al., 2015; Sturrock et al., 2015; Sakamoto et al., 2017; Chung et al., 2023), allowing for a range of retrospective biochemical assessments (Reis-Santos et al., 2023). While human bones are analysed in forensic pathology to elucidate drug use during the patient's life (Fernandez-Lopez et al., 2019), archival tissues have been rarely used for ecotoxicological applications, given that most exhibit low protein and lipid content, which is typically where contaminants bind.

Eye lenses are metabolically inert, incrementally grown, proteinaceous structures (Tzadik et al., 2017) which are formed of fibre cells laid down in concentric laminae (layers) (Fig. 1), with cells in the core formed during embryonic development and new laminae added sequentially as the fish grows (Bloemendal et al., 2004). The lens continues to grow by adding layers throughout the vertebrates' life but slows down with age, resulting in a near-isometric relationship between lens diameter and body size (Bron et al., 2000). During fibre cell differentiation, soluble proteins known as crystallins are produced (Bloemendal et al., 2004), then during the final stage of differentiation cells undergo a process similar to early apoptosis resulting in the degradation of organelles such as nuclei, mitochondria and ribosomes (Bassnett and Beebe, 1992). This creates the lens's transparency and removes its ability to synthesise or degrade proteins, rendering the structure metabolically inert (Bassnett and Beebe, 1992; Bloemendal et al., 2004). Further, the lens is not vascularised as it is entirely enclosed by the basement epithelial membrane. Consequently, ageing cells cannot be shed (Lynnerup et al., 2008), and the lens is not remodelled during the individual's life and the crystallins persist permanently.

Accordingly, eye lenses are becoming an increasingly popular target for life-history reconstructions, using stable isotope ratios of sequential laminae to track the movement and diet of the individual fish (Wallace, Hollander and Peebles, 2014; Peebles and Hollander, 2020; Young et al., 2022). Trace metals (Dove and Kingsford, 1998) and chronologies of heavy metal concentrations such as mercury have been measured in fish eye lens laminae (Miraly et al., 2023), but organic pollutants such as pharmaceuticals, pesticides and polycyclic aromatic hydrocarbons (PAHs) have not yet been quantified in this tissue. Eye lenses have particular advantages over otoliths for trophic and pollution reconstruction because they are made primarily of crystallin protein, but also contain lipids (Kuntz et al., 2024), and so lipophilic organic pollutants are more likely to partition into the matrix. Conversely, otoliths are almost entirely composed of calcium carbonate crystals, meaning that they primarily record ions that substitute for calcium (Campana, 1999). Otoliths do contain an organic matrix, but this contains no to negligible traces of lipids, reducing opportunities for them to record lipophilic pollutants. The organic matrix is composed of about 50% proteins, 30% proteoglycans, and 20% collagens (Borelli et al. 2001), but represents such a low fraction of the otolith mass (0.1–10%, but typically $< 1\%$; Degans et al. 1969) that it is challenging to use otoliths for trophic reconstructions (McMahon et al., 2011), and they often exhibit variable results for recording heavy metal exposure (Sturrock et al., 2012).

As the first step in developing the use of eye lenses in lifetime pollution exposure reconstruction, the main aim of this study was to assess whether teleost eye lenses can capture organic pollutants. There is

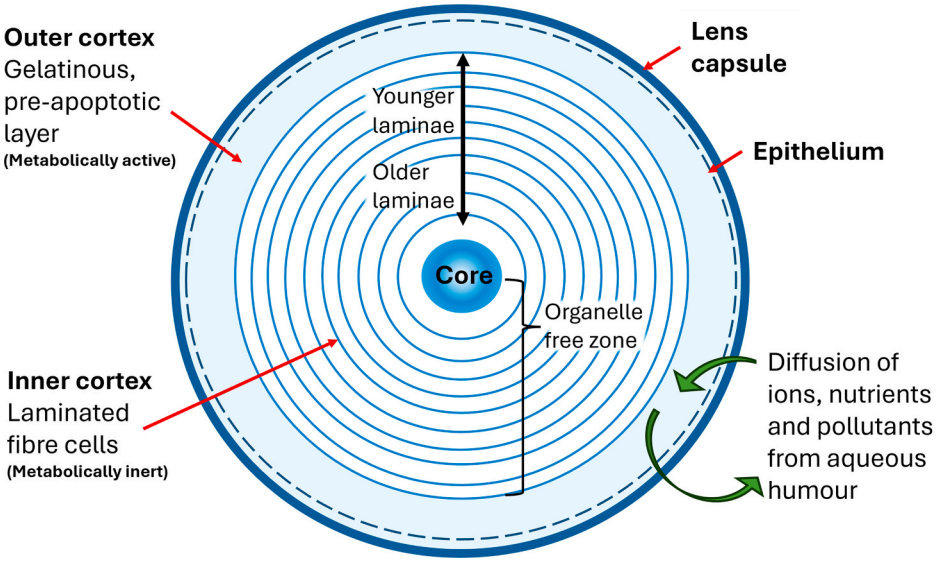

Fig. 1. Diagram of fish eye lens structure.

currently very limited data available in the literature on lipid content of fish eye lenses, so this was confirmed by weighing hexane-extracted lipids of fish eye lenses. The liver is a known pollutant sink due to its lipophilicity and role in metabolism and therefore acted as a positive control against which the chemical burden of the lens could be compared. Methods for the homogenisation and extraction of pollutants from eye lenses were optimised, and gas chromatography tandem mass spectrometry (GC–MS/MS) used to assess contaminant presence and concentrations in the different tissues. Additionally, we examined whether contaminant burden was associated with fish health (inferred using hepatosomatic index and Fulton's condition index). We focused on two teleost species sampled from marine and freshwater habitats: the common dab *(Limanda limanda*) and European eel (*Anguilla anguilla*). Dab are a flatfish commonly used as a bioindicator of sediment pollution due to their wide distribution and high prevalence of pollutant-associated diseases (Rijnsdorp et al., 1992). European eels are a catadromous species (Belpaire et al., 2019) that are critically endangered (IUCN, 2013) due to migration barriers, habitat degradation, and pollution (Jacoby et al., 2015). Their high fat content enhances pollutant accumulation, and the subsequent breakdown of their fat tissues during long distance spawning migrations can impair reproductive organs and gametogenesis (Belpaire et al., 2019).

2. Methods

2.1. Fish sampling and condition indices

Common dab (*Limanda limanda)* were trawled in July 2024 for this study as part of CEFAS' Clean Seas Environment Monitoring Programme (CSEMP) (n = 10, TL = 15.9——18.9 cm) from Liverpool Bay in the Celtic Sea (survey number CEND1224), approved by the University of Essex Ethics Committee (application no. ETH2324-1132). Fish were frozen at −20°C then dissected and subsampled at the University of Essex. Livers and whole eyeballs were stored in plastic Eppendorf tubes at −20°C. Silver European eels (*Anguilla anguilla)* were sampled in the River Haven, South Lincolnshire river by a commercial eel fisher as part of a project led by the Institute of Zoology (n = 10, TL = 35.0——57.8 cm), subject to ethical approval by the Zoological Society of London Ethics Committee (ethics no. IOZ192). Procedures were undertaken within licensed animal facilities (Establishment Licence XBABDAACB) by licensed animal technicians in conjunction with registered zoo veterinary surgeons with experience in fish medicine. Eel eyeballs were stored in plastic tubes and livers in aluminium foil at −20°C. For both species, prior to chemical extraction, whole lenses were dissected from the eyeball and then weighed. Anterior sections of liver (0.3 g) were cut using a scalpel. Lenses and liver subsamples were stored in Eppendorf tubes at −20°C until the day of chemical extraction. To infer fish condition and health, Fulton's condition factor (*K*) and hepatosomatic index (HSI) were measured prior to any tissue subsampling as $TW/TL^3 \times 1000$ and LW/TW × 100, respectively, where TW represents total weight in grams, TL represents total length in cm, and LW represents liver weight in grams.

2.2. Chemical extraction

The eye lens is a particularly rigid matrix, especially compared to standard biota matrices such as liver and muscle, and hence the first challenge was in selecting the most effective tissue homogenisation technique. For chemical extraction, samples were defrosted and four different extraction methods were tested, with one whole lens per extraction (mean mass dab eye lenses 0.02 g ± 0.01 g; eel eye lenses 0.02 g ± 0.006 g). Prior to each method trialled, each sample was spiked with 100 μl of the 1 ppm internal standard mix, vortexed for 5 S using a vortex mixer (ISG), and incubated in the dark for 15 mins. For the internal standards, a deuterated PAH mix was purchased from LGCStandards and diluted in hexane. Separately, a C13 labelled PCB mix in nonane was purchased from CK isotopes limited and diluted in hexane. Stock solutions were kept at −20°C for 6 months.

2.2.1. QuEChERS

The first method was a modified form of the QuEChERS method (quick, easy, cheap, effective, rugged and safe), a popular method for tissue extraction using food and environmental samples, adapted from (Anastassiades et al., 2003). 0.4 g of Original QuEChERS extraction salt (Agilent) was added to the tissue lysing tube containing the sample, internal standard, and ceramic sphere, along with 0.67 ml ultrapure water and 0.63 ml acetonitrile. Samples were shaken on the tissue lyser for 2 x 45 S at 7500 rpm (Precellys Evolution homogeniser, Bertin instruments) and centrifuged at 4000 RCF for 5 mins using a Harrier centrifuge (Sanyo). The contents were transferred to a centrifuge tube and 4.13 ml ultrapure water and 7.17 ml acetonitrile were added. Tubes were then vortexed for 5 S and centrifuged at 4000 RCF for 5 mins. The acetonitrile layer was transferred to the fatty sample dSPE 15 ml tube for lipid removal, vortexed 10 S and centrifuged again at 4000 RCF for 5 mins.

2.2.2. Smedes and Ultra-Turrax

The remaining methods utilised the Smedes method (Smedes, 1999) (hexane and isopropanol), but with different homogenisation techniques. The IKA™ ULTRA-TURRAX™ T 18 Digital Disperser (FisherScientific) was used to homogenise one sample in 6 ml HPLC grade hexane, 3 ml HPLC grade isopropanol (FisherScientific), and 1 ml ultrapure water (purified using a Milli-Q system), and thoroughly cleaned between samples with hexane, ultrapure water and Kimwipes (FisherScientific). After allowing the solution to separate, the organic phase was transferred to a centrifuge tube.

2.2.3. Smedes and pestle

Alternatively, samples were manually homogenised using a glass pestle in a boiling tube with 1 ml hexane and 1 ml isopropanol. The pestle was thoroughly cleaned between samples using ultrapure water, hexane and Kimwipes. The sample was then sonicated for 20 min, and 3 ml hexane, 1 ml isopropanol and 1 ml ultrapure water were added. Sample was vortexed one more time for 10 S and allowed to separate, after which the organic phase was transferred to a centrifuge tube.

2.2.4. Smedes and tissue lysing beads

The final method combined the Smedes method with tissue lysing tubes containing Lysing Matrix A (garnet flakes and a ceramic bead) (MP Biomedicals™). One tube contained one sample and 900 μl hexane and 500 μl isopropanol and shaken vigorously on the homogeniser for 2 × 45 S at 7500 rpm. Samples were then transferred to centrifuge tubes. The tissue lysing tubes were rinsed with 4 ml hexane, 2 ml isopropanol and 1 ml ultrapure water. Centrifuge tubes were vortexed again for 10 S each and centrifuged at 2000 RCF for 5 mins and the organic phase transferred.

2.3. Final clean-up and concentration

All liver sample extracts were cleaned using 6 ml columns (Macherey-Nagel™ CHROMABOND™) filled with 0.9 g anhydrous magnesium sulfate (ThermoScientific), 0.9 g silica gel (ThermoScientific) and 1.9 g alumina B – Super I (MP Biomedicals™). Columns were held in a Visiprep™ manifold cover (Supelco), pre-conditioned with hexane and then rinsed with 20 ml hexane after the samples had passed through. This clean-up stage was not included in lens extraction as pilot studies have shown lower levels of lipids in the extraction and this process introduced more background contamination. Finally, liver and eye sample extractions were evaporated down to 1 ml using the TurboVap (Biotage) and a gentle nitrogen gas flow at 40°C.

2.4. GC–MS/MS conditions

First, untargeted screening via GC–MS/MS was conducted to generate a list of tentative pollutants using a Shimadzu Nexis GC-2030 coupled to a GCMS-TQ8040 NX triple quadrupole mass spectrometer at the University of Essex. Automated injections were performed using an AOC-6000 (Shimadzu) with an LS 2 syringe tool. Solvent prewashes were performed using 3 x 8 μL isopropanol and post-washes used 3 x 8 μL hexane. 1 μL samples were injected under splitless mode with helium as a carrier gas, under a total flow of 10.1 ml/min and column flow of 1.27 ml/min. The oven was heated following the program in Table S1. The column was an Rtx®-5MS capillary column, 30 m in length and 0.25 mm internal diameter, 0.10 um film with 5 m Integra-Guard® (Restek, USA). The ion source temperature was 230°C and the interface temperature was 290°C. After 3 min, Q3 full scan mode was used to collect spectra from 50 – 500 *m/z*.

Second, single ion monitoring (SIM)-analysis was performed using Q1, focusing on the most abundant pollutant class observed in the untargeted screen (PAHs; ions listed in Table 1). For this, the same oven program was used as above. Finally, due to the known heavy industrial pollution of Liverpool Bay (Hawkins et al., 2020) and sediment and biota data reporting high levels of polychlorinated biphenyls (PCB) contamination in the Celtic Sea (Marine Directorate et al., 2025), SIM analysis targeting PCBs in dab eye lens and livers was also conducted. For this, the samples were injected under high pressure (10kPs at 1 min). Compound identification for target PAHs and PCBs was based on the reference peaks and retention time of external standards, and quantitation was based on the base peak, shown in Table 1.

2.5. Data processing

Obtained spectra were processed using LabSolutions postrun analysis software (GCMSsolution Version 4.50 SP1, Shimadzu, 2018). For the untargeted screen, peaks were automatically integrated and identified using components of the NIST mass spectral and retention index database. Only those with a minimum similarity of 80% and peak area > 5 × background were reported, and isomers or highly similar compounds were grouped together and given standardised names.

During SIM analyses, concentration was calculated using an external solvent calibration curve, corrected for recovery of the internal standards and normalised for sample mass (wet weight). PAH mixture 163 (LGCStandards) and QTM PAH mix (SigmaAldrich) were dissolved in hexane to make stock solutions, which were then combined and subsequently diluted again to make working concentration solutions for the external standard calibration curve (5 calibration levels from 5 − 100 ppb). For the PCB external standards, PCB-Mix 19 (LGCStandards) was also diluted in hexane to make a stock solution, which was used to make a 6-level calibration curve (25–500 ppb). Liver mass was calculated as total wet weight, not lipid weight, and so a direct comparison of concentration between tissue types cannot be drawn, only overall trends. Comparisons in PAH type can be drawn between matrices, and relative concentrations between compound type. Values above the limit of quantification (LOQ) but below the limit of detection (LOD) were allocated a value half of the compound-specific LOQ.

2.6. Validation and quality assurance

As part of the SIM analysis of targeted PCBs and PAHs, linearity was

Table 1
Target compound base peaks, reference ions, limit of detection (LOD = 3.3 × Response Factor standard error/slope of the calibration curve), limit of quantification (LOQ = 10 × Response Factor standard error/slope of the calibration curve) and linearity (presented as R^2 values for the calibration curves) achieved during SIM analysis, all calculated using external standards.

Contaminant class	Compound	Base peak *m/z*	Reference ions	LOD (ppb)	LOQ (ppb)	R^2 value
PAH	Naphthalene	128	127, 129	1.38	4.17	0.988
PAH	Naphthalene, 2-methyl-	142	141, 115	1.40	4.25	0.984
PAH	Naphthalene, 1,6-dimethyl-	156	141, 155	1.34	4.05	0.983
PAH	Acenaphthylene	152	151, 150	1.37	4.15	0.981
PAH	Acenaphthene	153	154, 152	1.35	4.09	0.979
PAH	Fluorene	165	166, 164	1.37	4.15	0.969
PAH	9H-Fluorene, 9-methyl-	165	180, 178	1.35	4.09	0.975
PAH	Phenanthrene	178	176, 152	1.38	4.18	0.952
PAH	Anthracene	178	176, 179	1.32	4.01	0.972
PAH	Dibenzothiophene	184	139, 152	1.32	3.99	0.974
PAH	9H-Fluorene, 2,3-dimethyl-	179	194, 178	1.31	3.98	0.966
PAH	1-Methyldibenzothiophene	198	197, 165	1.35	4.08	0.971
PAH	1,7-Dimethyldibenzothiophene	212	211, 197	1.35	4.08	0.972
PAH	Anthracene, 1-methyl-	192	191, 189	1.38	4.19	0.963
PAH	Fluoranthene	202	200, 203	1.34	4.06	0.970
PAH	Pyrene	202	200, 101	1.34	4.07	0.977
PAH	9,10-Dimethylanthracene	206	191, 205	1.49	4.50	0.974
PAH	Benz(a)anthracene	228	226, 229	1.38	4.18	0.969
PAH	Chrysene	228	226, 113	1.35	4.08	0.996
PAH	Benzo(b)fluoranthene	252	250, 126	1.41	4.28	0.986
PAH	Benzo(k)fluoranthene	252	126, 250	1.34	4.07	0.982
PAH	Benzo(e)pyrene	252	250, 125	1.36	4.13	0.981
PAH	Indeno(1,2,3-cd)pyrene	276	239, 137	1.49	4.51	0.987
PAH	Benzo(ghi)perylene	276	274, 137	1.38	4.19	0.984
PCB	PCB 18	186	256, 258	1.57	4.75	0.998
PCB	PCB 28	256	258, 186	1.56	4.73	0.997
PCB	PCB 44	292	290, 255	1.57	4.75	0.997
PCB	PCB 52	292	255, 150	1.56	4.74	0.998
PCB	PCB 101	326	254, 127	1.57	4.75	0.997
PCB	PCB 149	360	362, 290	1.59	4.81	0.998
PCB	PCB 118	326	328, 324	1.58	4.80	0.998
PCB	PCB 138	360	362, 290	1.58	4.80	0.998
PCB	PCB 153	360	362, 290	1.59	4.82	0.998
PCB	PCB 180	394	396, 324	1.63	4.94	0.999
PCB	PCB 170	394	396, 324	1.61	4.89	1.000
PCB	PCB 194	430	428	1.61	4.86	0.995

assessed using the correlation coefficient (R^2) values of the external calibration curves. LOD was calculated based on 3.3* Response Factor standard error/slope of the calibration curve, and LOQ on 10* Response Factor standard error/slope of the calibration curve (Table 1) (Dolan, 2021). Both were calculated in the absence of other contaminants, but no interference was later found as there was no overlap in retention time or quantifying ions between analytes and non-target contaminants. LOD/LOQ were tested using external standards at around the estimated LOD and LOQ to confirm that signal:noise was acceptable. Samples were spiked with internal standards prior to homogenization in order to quantify recovery (Table 2).

To ensure quality control, the column was pre-conditioned at the start of each batch with a sample, before running a standard calibration curve. Solvent blanks were also run after the calibration curve, every 3 samples, and at the end of the batch to ensure no carryover of analytes. Samples were analysed in batches of 10 to also reduce the chance of carryover or drifting of analyte retention times, beginning with a spiked process (procedural) blank to account for any laboratory-based contamination. Precision was checked using daily triplicate injections of labelled solvent standards and the relative standard deviation (RSD) of the peak areas measured for each target analyte (Table 2). To monitor quality assurance, linearity of external standards and recovery of internal standards were monitored across batches. The instrument was also auto-tuned once a week and after any maintenance.

2.7. Eye lens lipid content determination

For lipid content determination of the eye lenses, one whole lens (capsule on; i.e. reflecting the matrix used for contaminant analyses in the study) from each of four individuals were pooled per sample (n = 3 for dab, n = 2 for eels) and extraction was performed using tissue lysing beads and the Smedes method described above. As we also had the second lens for these dab, we removed their capsules and repeated the experiment to assess whether this modified the outcome. The organic phase was then allowed to evaporate to dry and the lipid residue weighed.

Table 2
Precision and recovery values for each internal standard. Precision is given as relative standard deviation (RSD %), based on peak area of labelled (internal) solvent standards injected in triplicate per species and day. Recovery % is given as mean values for liver and eye lenses for each species (PCBs not analysed in eel tissue).

Chemical class	Compound	Mean RSD (%)	Mean recovery (%)			
			Eel eye lens	Eel liver	Dab eye lens	Dab liver
PAH	Naphthalene-D8	2.08	44.67	63.01	45.95	64.99
PAH	Acenaphthylene-D8	2.06	49.11	56.56	45.70	63.42
PAH	Acenaphthene-D10	1.64	52.37	58.37	46.50	65.33
PAH	Fluorene-D10	1.88	54.08	60.22	46.34	68.92
PAH	Phenanthrene-D10	1.57	60.37	59.93	47.28	70.01
PAH	Anthracene-D10	1.63	60.28	63.49	46.68	72.03
PAH	Fluoranthene-D10	2.36	67.73	60.32	49.18	69.22
PAH	Pyrene-D10	2.08	68.15	66.19	48.76	68.71
PAH	Chrysene-D12	1.79	69.94	58.95	52.09	58.29
PAH	Benzo(b) fluoranthene-D12	2.15	77.20	56.25	52.27	46.04
PAH	Benzo(k) fluoranthene-D12	1.38	59.84	53.08	52.86	41.51
PAH	Benzo(a)pyrene-D12	2.20	65.70	49.57	54.08	43.66
PAH	Indeno(1,2,3-c,d) pyrene-D12	1.95	72.90	51.62	54.05	42.13
PCB	PCB28-13C	1.69	NA	NA	53.64	69.06
PCB	PCB52-13C	1.11	NA	NA	53.19	64.89
PCB	PCB101-13C	1.34	NA	NA	53.36	66.16
PCB	PCB138-13C	1.81	NA	NA	53.51	112.12
PCB	PCB153-13C	2.39	NA	NA	53.60	63.02
PCB	PCB180-13C	2.60	NA	NA	55.11	67.90

2.8. Statistical analyses

All analyses were undertaken in R version 4.3.2 (R Core Team, 2023). Linear regression was used to explore relationships between total PAH concentrations in liver vs. eye lenses from the same fish to investigate patterns in chemical abundance between tissues. Linear regression was also used to test for relationships between condition indices (K and HSI) and total PAH content of each tissue. For every pairwise test, residuals were checked for normality and equal variance, and variables were logged if necessary to meet these assumptions. In cases where the data could not be transformed to meet assumptions of equal variance, Pearson's correlations were performed.

To explore differences in PAH profiles among tissues and species, concentration data were log(x + 1)-transformed to reduce skewness while retaining zero values, and then centred and scaled prior to analysis. Principal components were calculated using the prcomp function in R. Differences in multivariate PAH composition among species and tissue types were assessed using permutational multivariate analysis of variance (PERMANOVA) implemented with the adonis2 function in the vegan package. Analyses were based on Euclidean distance matrices calculated from the log(x + 1)-transformed concentration data. Homogeneity of multivariate dispersion was evaluated using the betadisper function in the vegan package.

3. Results

3.1. Comparison of homogenisation and extraction methods

The results of the different methods trialled are summarised in Table 3. Most notably, although it is a popular method for the quantification of organic pollutants in environmental samples, QuEChERS could not reliably homogenise the eye lenses. Despite complete homogenisation of the liver, recovery of the spiked internal standards was still consistently lower than the other methods trialled (namely, the Smedes method). Therefore, acetonitrile and QuEChERS salts were rejected.

The lenses were too small for the Ultra-Turrax digital disperser and cleaning the tool between samples proved challenging due to adherence of the gelatinous cortex, resulting in cross-contamination. Therefore, accurate recovery values for the spiked internal standards could not be obtained, this tool was rejected and Fig. 2 only presents recovery rates for the other three methods.

The tissue lysing matrix with one sample per tube proved the most effective homogenisation methods whilst minimising the risk of cross-contamination. This technique was also compared against the use of a glass pestle, but this tool proved more time-consuming and less effective. The effect of the different homogenisation techniques on recovery of spiked internal PAH standards in eel liver samples is shown in Fig. 2; lysing beads combined with the Smedes method gave the most consistent and often highest recovery of spiked internal standards and so was selected as the finalised method. However, there were notable declines in recovery rates of 5-ring PAHs in the eel livers (Fig. 3).

3.2. Contaminants in different tissue types indicated by untargeted screens

Results of the untargeted screen conducted in full scan mode are reported in Table 4. Most notably, PAH derivatives were found in almost every liver subsample in both eel and dab, but not in the paired lenses.

Additionally, benzoic acid, 3-amino-, ethyl ester (also known as MS-

Table 3
Results of different tissue homogenisation and solvent extraction techniques trialled for GC–MS/MS analysis of PAHs in whole fish eye lenses. Asterisk = chosen method; § = background contamination controlled for using a process blank.

Goal	Tried methods	Results
Complete tissue homogenisation	Ultra-Turrax	Lenses got trapped in blades and did not homogenise. The tool was also difficult to effectively clean between samples and risked cross-contamination.
	Glass pestle and boiling tube	Very time consuming; lens too rigid for easy homogenization.
	Tissue lysing matrix (garnet flakes and ceramic beads) *§	**Complete homogenization with no cross-contamination. Some background contamination introduced from the plastic tube.**
Chemical extraction with maximum recovery	QuEChERS	Incomplete homogenisation resulted in poor and variable recovery rates. Also missed some PAHs that were found in the same sample using Smedes.
	Smedes reaction *	**More consistent recovery rates. Combination of a polar and non-polar solvent helped with complete homogenisation and separation of the organic phase.**
Sample clean-up of lens extractions to reduce background noise	Silica/ alumina/ magnesium sulfate column	Effectively removed lipids from the sample, but reduced recovery and introduced more background contamination than it removed.
	Centrifugation *	**Reduced amount of solid matter in the final extraction by forcing it into the pellet, reducing the chance of sample cross-contamination within the instrument.**
	No follow-up clean-up step	No improvement in internal standard recovery but increased risk of accidental injection of solid matter into the instrument (reducing instrument insert lifespan and increasing chance of cross-contamination).

222) was found in every eel eye lens. This was the anaesthetic used to terminate the eels during sampling by submersion in a dosed water bath. The detection of this compound during the untargeted screen confirms that a) that chemicals in the surrounding media can indeed be sorbed onto or into eye lenses and b) the untargeted screening system works as it successfully detected a known compound that the fish had been exposed to in the water, but which had not been targeted in analysis.

3.3. Relationships between total PAH concentrations among tissues and with fish condition indices

The total concentration of all PAHs which were targeted by SIM were positively correlated between the liver and eye lenses from the same individual in both species, but the relationship was only significant for eels ($P = 0.024$; Fig. 4). None of the relationships between condition indices (HSI and K) were significant (Fig. 5, Fig. S1), but there was some suggestion of a weak positive correlation between HSI and the sum PAH concentrations in the dab livers and eye lenses, but negative or no relationships for the eels (Fig. 5).

3.4. Differences in PAH types found in each tissue

While a range of PAHs (up to five different compounds per individual and tissue type) were detected in both the eel and dab livers during SIM analysis, only four were found in the eye lenses (two per species) (Fig. 6). In the eel eye lenses, naphthalene was the only PAH above the SIM LOQ: the lowest molecular weight and least lipophilic PAH of those targeted (pyrene was detected but < LOQ in one sample). Both pyrene and naphthalene were also quantifiable in eel liver samples, but pyrene was much more commonly detected in liver samples (Fig. 6).

In dab, dibenzothiophene and chrysene were the only PAHs > LOD or LOQ in eye lenses, neither of which could be detected in dab liver samples during SIM analysis (Table S3). There is no clear correlation between the tissue type and the molecular weight or lipophilicity of the PAHs detected in them.

The PCA showed clear among-species differences in PAH profiles, with most of the differences driven by liver loadings, given sparse eye lens data (Fig. S3). However, the PERMANOVA, indicated significant differences in PAH composition, both among tissues ($R^2 = 0.144$, $F = 6.04$, $p = 0.002$) and species ($R^2 = 0.118$, $F = 4.80$, $p = 0.002$), and when included in the same model, species and tissue type explained 26.1% of the variation in PAH composition ($R^2 = 0.261$, $F = 6.19$, $p = 0.001$). However, tests for homogeneity of multivariate dispersion were also significant ($p < 0.05$ for both covariates), signaling differences in within-group variability and suggesting that these PERMANOVA results should be interpreted with caution.

3.5. Differences in the number of PCBs found in each tissue

As Fig. 7 shows, the optimised GC–MS/MS parameters achieved acceptable recovery for spiked C13 internal PCB standards for both liver and lens samples, but no PCBs were detected in lenses. Conversely, PCBs 101, 118, 138, 149, 153, 18, 180, and 28 were quantifiable in the liver samples, with up to 8 congeners (out of the targeted 14) found in a single fish.

3.6. Lipid content of fish eye lenses

Although the levels were variable, lenses were confirmed to contain lipids, and eel eye lenses contained 1.79 times more lipid on average than dab eye lenses (Table 5). Removal of the lens capsule had very little impact on the lipid content, suggesting most of the lipids were in the cortex and core of the lens.

4. Discussion

In this study, we successfully developed methods for the extraction and measurement of organic pollutants in the eye lenses of common dab and European eel using GC–MS/MS. Fish eye lenses have previously been used to infer past habitat use (Young et al., 2022), diet (Bell-Tilcock et al., 2021) and trophic shifts (Wallace, Hollander and Peebles, 2014) using stable isotope chronologies, and heavy metal exposure using copper (Dove and Kingsford, 1998) and mercury (Miraly et al., 2023) concentration profiles. However, to our knowledge, the present study is the first to detect organic pollutants in fish eye lenses. As we were generally close to detection limits for the current method, we did not attempt to subsample lenses in order to analyse pollutants at the lamina-level and the methods presented here will need to be further refined to achieve lifetime exposure reconstructions. Specific suggestions for these modifications are outlined in Section 4.7 Future directions. However, total PAH concentrations in whole lenses were positively related to liver concentrations from the same fish, suggesting that chronological pollutant exposure histories could be a possibility in the future.

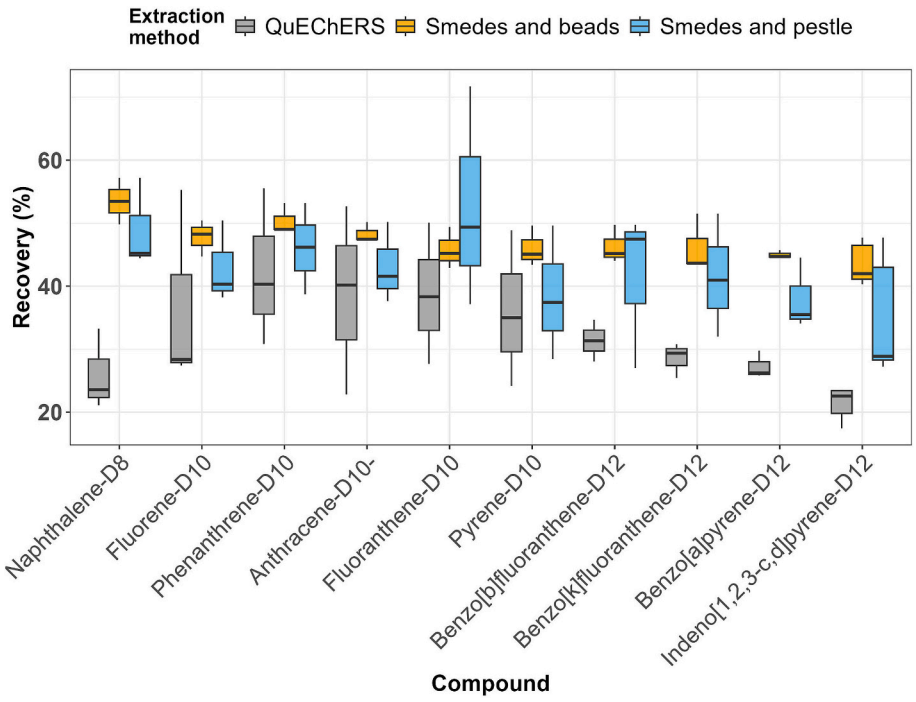

Fig. 2. Effect of different tissue homogenisation and extraction methods on recovery of spiked deuterated PAH standards in eel liver subsamples. Eye lenses were not successfully homogenised by QuEChERS and so recovery could not be compared. Boxes represent the interquartile range (IQR), with the centre line indicating the median. Whiskers extend to the most extreme value within 1.5 × IQR.

Interestingly however, different types of PAHs were found in lens and liver tissues, suggesting different pathways and affinities among tissue types, as discussed below.

4.1. PAHs can be effectively recovered from fish eye lenses and broadly relate to liver concentrations

The main environmental organic pollutants identified in the livers via untargeted GC/MS-MS analysis were polycyclic aromatic hydrocarbons (PAHs) and PAH derivatives. While the same compounds were rarely observed in the untargeted screening of paired lenses, it was assumed that this was due to low concentrations and insufficient sensitivity of the analysis method. As such, we subsequently performed a PAH-targeted SIM analysis, the improved sensitivity of which was able to detect and quantify the low PAH concentrations in tissues with very low concentrations, including fish eye lenses. In particular, naphthalene, which was indicated in 50% of the dab liver samples by the untargeted screen, was then quantified in 70% dab livers, one eel liver, and 60% of eel eye lenses.

PAHs are semi-volatile, persistent organic pollutants derived from petroleum products (petrogenic), the burning of fossil fuels or biomass (pyrogenic), or biogenic sources (the transformation of natural organic precursors; e.g. perylene and naphthalene) (Neff, Stout and Gunster, 2005). PAHs containing two – three rings are considered light, while those with four or more are considered heavy, and are more stable, lipophilic, and toxic (Lawal, 2017).

While not a strong relationship, total PAH concentrations in the liver and lens from the same fish were consistently positively correlated, both in dab (albeit non-significantly) and eels. This provides some confidence in the potential for eye lenses to be used as recorders of organic pollutants, with the most contaminated animals exhibiting the highest PAH concentrations in both tissues. However, there were multiple dabs with intermediate to high levels of liver burden but no PAHs above detection limits in the paired lenses, suggesting that these individuals were either exposed to a specific suite of PAH types not accumulated in eye lenses (see below) or that our current extraction and/or analysis methods need further refinement.

We had expected total PAH concentrations to be negatively correlated with fish health indices (inferred by HSI and K), but all correlations were non-significant, and – for dab – if anything, the slopes tended to be positive. However, condition index and liver size are influenced by a range of factors (Bervoets and Blust, 2003; Ajani Ek and Olanrewaju An, 2015; Alloy et al., 2020; Hauser-Davis et al., 2021), and HSI can be positively related to pollution exposure, so the conflicting results are not necessarily surprising. For example, HSI was positively related to PAH exposure in adult brown bullheads (*Ameiurus nebulosus*) (Pinkney et al., 2001). HSI was also elevated in *Geophagus brasiliensis*, *Hypostomus affinis* and *Hypostomus auroguttatus* residing in sites contaminated by industrial and urban run-off due to increased hepatocyte production and/or hypertrophy relating to the increased detoxification demands (Morado, Araújo and Gomes, 2017).

4.2. Bioaccumulation rates of PAHs are highly compound- and species-specific

Tissue distribution of PAHs can be affected by PAH types and concentrations in the surrounding environment (e.g. water, diet, sediments), tissue lipid content, and metabolism, and hence is highly compound-, species- and life stage-specific. For instance, carp (*Cyprinus carpio)* exhibited greatest total PAH concentrations in the brain, while topmouth culter (*Culter eryropterus*) and bighead carp (*Aristichthys nobilis*) exhibited preferential bioconcentration in the gills and muscle (Qin et al., 2020). It is therefore not surprising that, in the present study, the concentration, number and types of PAHs detected in dab and eel eye lenses and livers varied by tissue type and species. Even within teleosts, metabolic capacity for different PAHs can vary significantly between species (Pulster et al., 2017). The differences in concentrations and types of PAHs observed here may thus be related to species-specific metabolism, as well as to different sources of PAHs between regions and/or between fresh and marine waters (Tobiszewski and Namieśnik, 2012; Mali et al., 2022).

The data presented here suggest no clear pattern for liver or lens

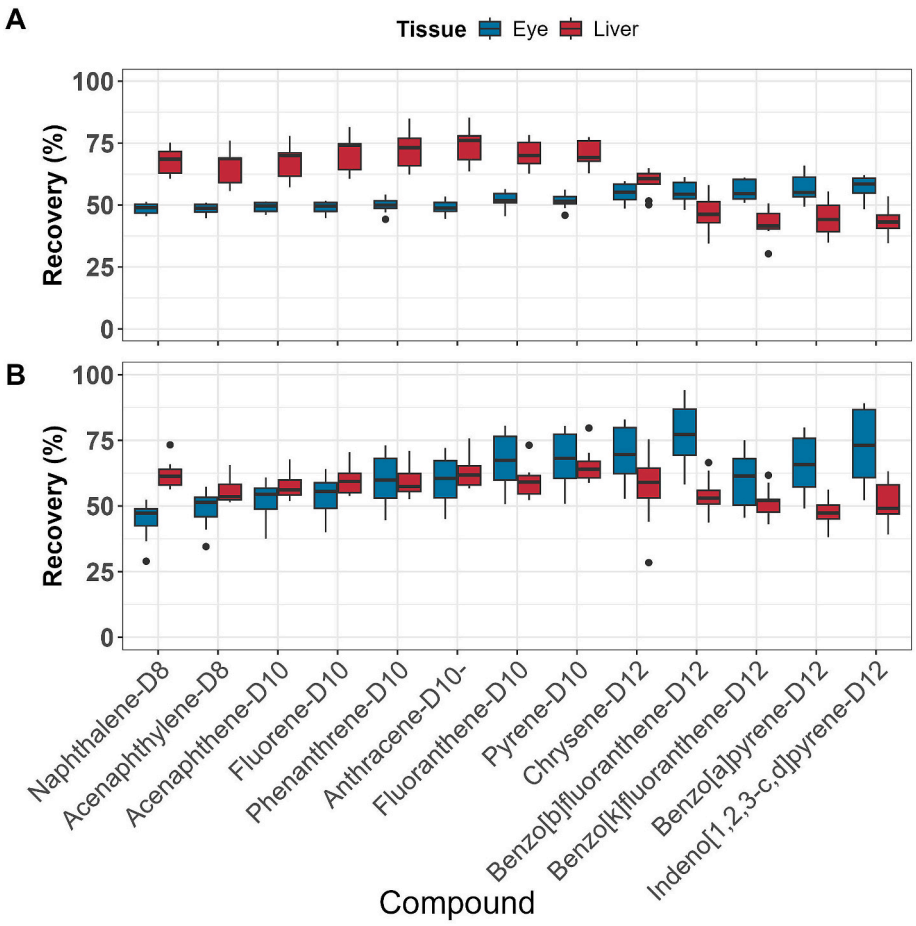

Fig. 3. Effect of matrix (liver compared with eye lens) on recovery of spiked deuterated PAH standards using the final chosen methods of lysing matrix beads and Smedes reaction, shown in (A) dab and (B) eel (n = 10 per species), and quantified using SIM analysis. The deuterated standards are shown in order of increasing molecular weight and lipophilicity from left to right. Boxes represent the interquartile range (IQR), with the centre line indicating the median. Whiskers extend to the most extreme value within 1.5 × IQR.

tissue to preferentially bind PAH types with higher molecular weight or lipophilicity. While this differs from some previous studies which compare PAH distribution in other fish tissues (Qin et al., 2020), this may reflect the considerable variation among tissue-specific processes, studies and species. In Qin et al. (2020), low molecular weight (LMW) PAHs dominated in the viscera of three teleost species, while medium and higher molecular weight (MMW and HMW, respectively) PAHs were detected at higher levels in the gills, which come into direct contact with contaminated particulate matter. However, Qin et al's (2020) study also reported that the tissue distribution of total PAHs varied between the three teleost species, suggesting species-specific toxicokinetics (Qin et al., 2020). In contrast, other studies suggest tilapia gills provide a more efficient uptake pathway via bioconcentration for LMW, less lipophilic, PAHs as opposed to highly lipophilic PAHs which entered via bioaccumulation resulting from ingestion, but this was impeded by enhanced biotransformation (Liang et al., 2007). The liver is the main site of PAH detoxification in fish, where most PAHs undergo phase I and phase II biotransformation, resulting in water-soluble conjugates to aid excretion (Van Der Oost, Beyer and Vermeulen, 2003). Therefore, although the liver is very lipid-rich, bioaccumulation of PAHs in this tissue is likely to be reduced by metabolism, the rate of which will vary between PAH types depending on their structure and bioavailability. Nevertheless, PAHs can bioaccumulate in the liver (Rahmanpour, Farzaneh Ghorghani and Lotfi Ashtiyani, 2014), particularly in bottom-dwelling fish which live in contaminated sediments (Honda and Suzuki, 2020), such as dab.

4.3. *Influence of PAH molecular weight and lipophilicity on recovery*

The recovery rates of internal standards in eye lenses were largely consistent across different PAHs, however recovery in liver samples decreased for the HMW PAHs in both dab and eel samples. In both species, the sudden drop in recovery in livers occurred at benzo(b)fluoranthene, the first 5-ring PAH of the standards. Generally speaking, HMW PAHs are more lipophilic than smaller, lighter PAHs (Honda and Suzuki, 2020) due to greater hydrophobicity resulting from the greater number of rings (Wang et al., 2024). Our recovery data therefore suggests that the spiked HMW PAHs sorbed more effectively to the more lipid-dense tissue (liver) in contrast to the lenses, resulting in lower recovery. The fact that PAH recovery in lenses did not drastically change with molecular weight suggests that lipid content of the lenses does not have an influence on the sorption of the compounds to the tissue. Interestingly, Wang *et al.* also found that PAH bioconcentration factors were unaffected by molecular weight. Therefore, for fish exposed to PAHs in the environment, the primary route of uptake in lenses is more likely to be bioconcentration (i.e., direct from the water) than bioaccumulation (via ingestion, sediment and water, etc.), which is more dependent on lipid content (Frapiccini et al., 2018).

4.4. *The low lipid content of eye lenses reduces pollutant bioaccumulation*

Overall, very few contaminants were quantifiable in dab or eel eye lenses. Untargeted analyses primarily detected plasticisers and PAH derivatives, but only a small selection of PAHs could subsequently be

Table 4
Results of an untargeted screen of livers and eye lenses for dabs and eels, showing the number of samples in which each compound was detected. The tentative compounds named are those which gave at least 80% similarity match in the NIST library, and for peaks that were more than five times the background area. ND = not detected.

Tentative Compound	Chemical Type	Potential Sources	Eel Eye N = 9	Eel Liver N = 10	Dab Eye N = 9	Dab Liver N = 10
17-Pentatriacontene	Alkene	Biogenic, or industrial	ND	1	ND	ND
Diphenylamine	Aromatic amine	Antioxidant, stabiliser, pesticide	ND	2	ND	ND
Isophthalic acid, octyl *trans*-hex-3-enyl ester	Aromatic diester	Plasticiser derivative	1	ND	ND	ND
1-Propoxypropan-2-yl benzoate	Aromatic ester	Personal care product, plasticisers	1	ND	ND	ND
ethanethioic acid, S-(2-methyl-5-benzoxazolyl) ester	Aromatic heterocyclic thioester	Pharmaceutical or pesticide derivative	ND	1	ND	ND
Benzoic acid ester	Benzoic acid ester	Personal care product	ND	2	ND	ND
Benzoic acid, 3-amino-, ethyl ester	Benzoic acid ester	Fish anaesthetic	9	ND	ND	ND
Propane, 1,2,3-trichloro-2-methyl-	Chlorinated alkane	Industrial solvent or pesticide derivative	ND	ND	ND	1
Trichloroacetic acid, hexadecyl ester	Ester	Personal care product	ND	3	ND	ND
Isopropyl myristate	Fatty acid ester	Personal care product	ND	9	ND	ND
Linoleic acid ethyl ester	Fatty acid ester	Personal care product	ND	8	ND	ND
4(1H)-Pyrimidinone, 5-bromo-	Halogenated pyrimidinone derivative	Pharmaceutical intermediate	ND	ND	ND	5
dl-Proline, 1-(phenylmethyl)-	N-substituted amine	Pharmaceutical derivative	5	ND	ND	ND
Tris(1,3-dichloroisopropyl)phosphate	Organophosphate	Flame retardant, pesticide, plasticiser	1	ND	1	ND
Naphthalene	PAH	Biogenic, petrogenic, or pyrogenic	ND	ND	ND	5
1-Methoxymethylfluorene	PAH derivative	Biogenic, petrogenic, or pyrogenic	ND	ND	ND	9
1-Phenanthrenecarboxaldehyde, 1,2,3,4,4a,9,10,10a-octahydro-1,4a-dimethyl-7-(1-methylethyl)-, [1R-(1.alpha.,4a.beta.,10a.alpha.	PAH derivative	Biogenic, petrogenic, or pyrogenic	ND	1	ND	ND
4b,8-Dimethyl-2-isopropylphenanthrene, 4b,5,6,7,8,8a,9,10-octahydro-	PAH derivative	Biogenic, petrogenic, or pyrogenic	ND	4	ND	ND
6,7-Dimethyl-1,2,3,5,8,8a-hexahydronaphthalene	PAH derivative	Biogenic, petrogenic, or pyrogenic	ND	10	ND	1
Naphthalene, 1,2,3,4-tetrahydro-1,1,6-trimethyl-	PAH derivative	Biogenic, petrogenic, or pyrogenic	ND	9	ND	1
Phenol, 2,4,6-tris(1-phenylethyl)-	Phenol	Plasticiser	ND	2	ND	ND
Tert-butylated phenol derivative	Phenol	Plasticiser, or analytical artefact	7	7	9	ND
Bis(2-ethylhexyl) phthalate	Phthalic acid	Plasticiser	ND	5	ND	ND
Isophthalate ester	Phthalic acid ester	Plasticiser	ND	ND	1	ND
Long chain phthalate diester	Phthalic acid ester	Plasticiser	1	5	1	2
Phthalate monoester	Phthalic acid ester	Plasticiser	ND	ND	ND	1
Short chain phthalate acid ester	Phthalic acid ester	Plasticiser	ND	1	ND	ND
Heptyl phthalate monoester	Phthalic acid monoester	Plasticiser derivative	ND	ND	ND	1
4H-Inden-4-one, 1,2,3,5,6,7-hexahydro-1,1,2,3,3-pentamethyl-	Polyalkylated cycloketone	Fragrance ingredient in Personal care products	ND	ND	ND	1
Adamantane, 1,3-dimethyl-	Polycyclic saturated hydrocarbon	Pharmaceutical derivative	ND	ND	ND	1
1-Hentetracontanol	Primary alcohol	Biogenic or natural pharmaceutical	ND	ND	ND	1
Alkyl-substituted thiazole	Substituted thiazole	Flavouring/fragrance ingredient	ND	1	ND	ND

quantified (i.e. > LOQ) using targeted SIM analysis. This was despite a wide diversity of PAHs quantified in the matching liver samples, confirming exposure of the fish to PAHs. We hypothesise that this is primarily the result of the low lipid content of eye lenses, for example we measured 3.5% (+/- 1.926%) in eel eye lenses, while 23.2% (+/- 6.9%) has previously been reported in the liver of European eels (Parzanini et al., 2021).. As a particularly lipid-rich tissue with a crucial role in metabolism and detoxification (Topić Popović et al., 2023), lipophilic pollutants often preferentially accumulate in the liver. For PAHs in particular, lipophilicity increases with molecular size while hydrophobicity decreases, hence aquatic animals tend to take up LMW PAHs directly from the water while HMW are more likely to accumulate via ingestion (Wang et al., 2024). While the lipid content of human lenses is well documented (Borchman and Yappert, 2010), less is known about lipid distributions in fish lenses, although the evidence suggests that their total lipid content is lower than in mammals (Kiss, Devries and Morgan-Kiss, 2010; Kuntz et al., 2024). The present study confirms that lipids are present in dab and eel eye lenses in low levels (averaging 1.95% in dab and 3.50% in eels, Table 5), particularly in the form of cholesterol (e.g. Fig. S2). However, these were not at high enough levels to merit post-extraction clean-up (a technique which, when trialled, introduced background contamination to the lenses but did not improve recovery of the analytes).

The low bioaccumulation potential of lenses was also reflected in the results of the polychlorinated biphenyls (PCBs)-targeted SIM analysis which confirmed that numerous PCBs, a highly lipophilic class of compounds, were present in dab liver samples, but none were detected in the comparatively lipid-poor eye lenses. This implies limited bioconcentration of PCBs from the water, and bioaccumulation was the primary route of PCB uptake. Since none were found in the eye lenses, this would suggest the PCBs were not transported to the lens layers during the nucleated phase while the outermost layers were being formed. This is in keeping with what is known about the properties of PCBs, which strongly bind to sediment and organic matter, are primarily

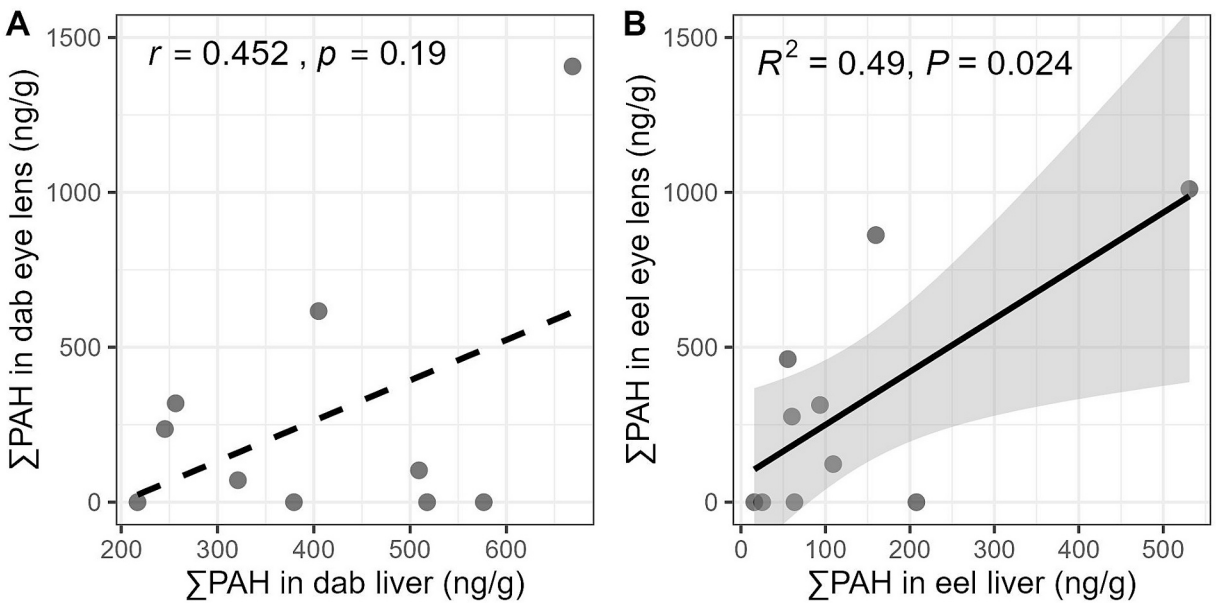

Fig. 4. Relationship between eye lenses and liver sum PAH concentration (measured by SIM) in the eye lenses and livers of (A) dab (dashed line shows simple linear fit; r and p values are from Pearson's correlation) and (B) eels (regression statistics shown on plot, grey area shows 95% CI).

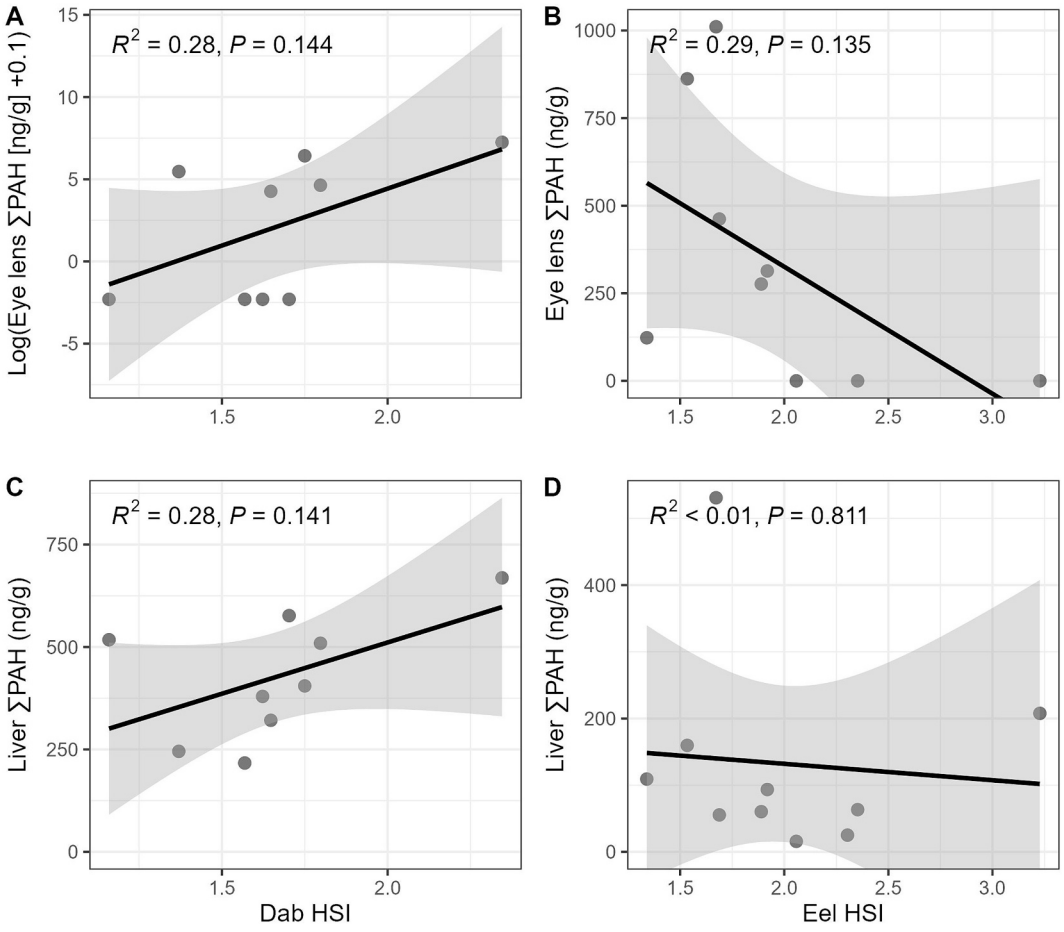

Fig. 5. Relationships between eye lens or liver total PAH concentrations (measured by SIM) and hepatosomatic index (HSI) of dabs and eels. (A) dab eye lens PAH concentration (log transformed) versus HSI; (B) eel eye lens PAH concentration versus HSI; (C) dab liver versus HSI; eel liver versus HSI. Note differing y-axes. (Regression statistics shown on each plot; grey areas show 95% CI).

ingested and recalcitrant to biotransformation (and hence easily bio-magnify within foodwebs) (James and Kleinow, 2014).

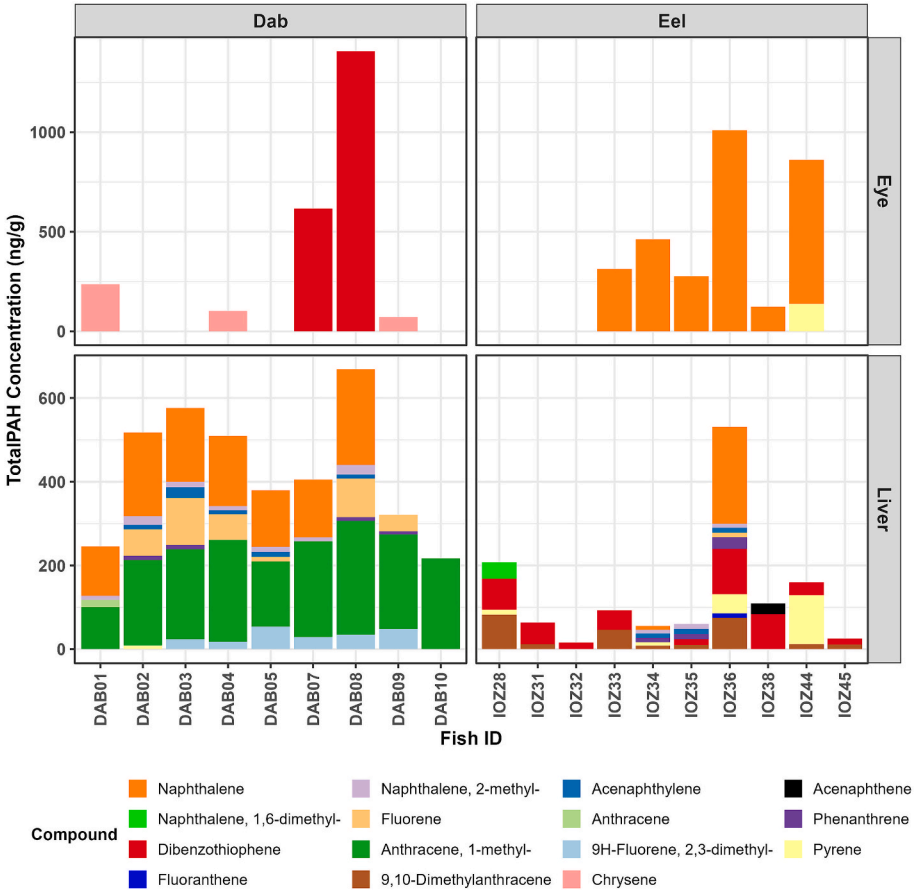

Fig. 6. Total PAH concentration in paired liver subsamples and eye lenses, shown for individual dabs and eels, coloured by PAH type. Compounds in the legend are listed in order of increasing molecular weight from left to right.

4.5. Eye lenses could reveal more about naphthalene exposure than conventional tissue analysis

The methods outlined here could not achieve lamina-level sensitivity to provide temporal resolution due to the very low pollutant concentrations, but the detection of chemicals within the whole lens can still provide helpful information. In the case of PAHs, routinely monitored tissue (e.g. muscle, liver) are not always reliable as indicators of PAH exposure due to rapid biotransformation (Van Der Oost et al., 1994) and so bile PAH conjugate concentration is a popular alternative, but even this can only indicate very recent exposure (Beyer et al., 2010). In contrast, the data presented here suggests that naphthalene was preferentially concentrated in the lens of eels over the liver, potentially linked to its properties as a less lipophilic LMW PAH. This illustrates the potential of the eye lens, as a metabolically inert tissue, to capture a signal of chemical exposure which would not be detected in standard tissues which have greater capacity for detoxification and excretion.

The ability to identify past exposure to PAHs is valuable as the metabolism of PAHs often results in reactive metabolites which can bind to, and damage, DNA, RNA and proteins. Hence, many PAHs are considered promutagenic or procarcinorgenic (Beyer et al., 2010). None of the individuals used in the present study appeared to be adversely affected by the low concentrations of PAHs detected, as indicated by a lack of significant correlation between HSI or condition index and chemical contamination, and no obvious deformities. However, the presence of PAHs in archival tissue does indicate potential environmental risk to the population. Chrysene, which was detected in several dab eye lenses, is one of the most persistent oil-derived PAHs in the water column, and can be oxidised to teratogenic derivatives, which have also been linked to eye deformities (Diamante et al., 2017).

4.6. Method development: Homogenisation and process blanks

The eye lens is a particularly rigid matrix, especially compared to standard biota matrices such as liver and muscle, and hence the first challenge was in selecting the most effective tissue homogenisation technique. Most notably, despite being a popular method for the quantification of PAHs in environmental samples (Khorshid et al., 2015), QuEChERS could not reliably homogenise the eye lenses. Additionally, despite full homogenisation of the liver, recovery of the spiked internal standards was consistently lower than the other methods trialled (namely, the Smedes method). Therefore, acetonitrile and QuEChERS salts were rejected. The Smedes method (hexane and isopropanol) was the most efficient when combined with the tissue lysing matrix; the use of one tube per sample allowed for simultaneous homogenisation on the tissue homogeniser (and therefore relatively high throughput) with minimum risk of cross-contamination. This contrasted with the alternatives which had lower throughput and higher risk of cross contamination, i.e., the Ultra-Turrax which was difficult to effectively clean, and the glass pestle which was labour-intensive.

As the chemical burden of lenses had not previously been characterized and it was unknown which, if any, pollutants could bind to this tissue, this study began as an untargeted screen and hence the Smedes method was also selected for its capacity to extract a broader range of chemical classes. The disadvantage is that this is not the optimal method for maximising the recovery of PAHs, unlike more established methods such as QuEChERS, and as such the analyte recovery rates achieved here are sometimes slightly below the rates deemed acceptable for environmental assessments (e.g. 50–150% for the US EPA (EPA, 8270 E, 2018)). However, this seminal work provides the groundwork for future research into the development of specific assays tailored for the

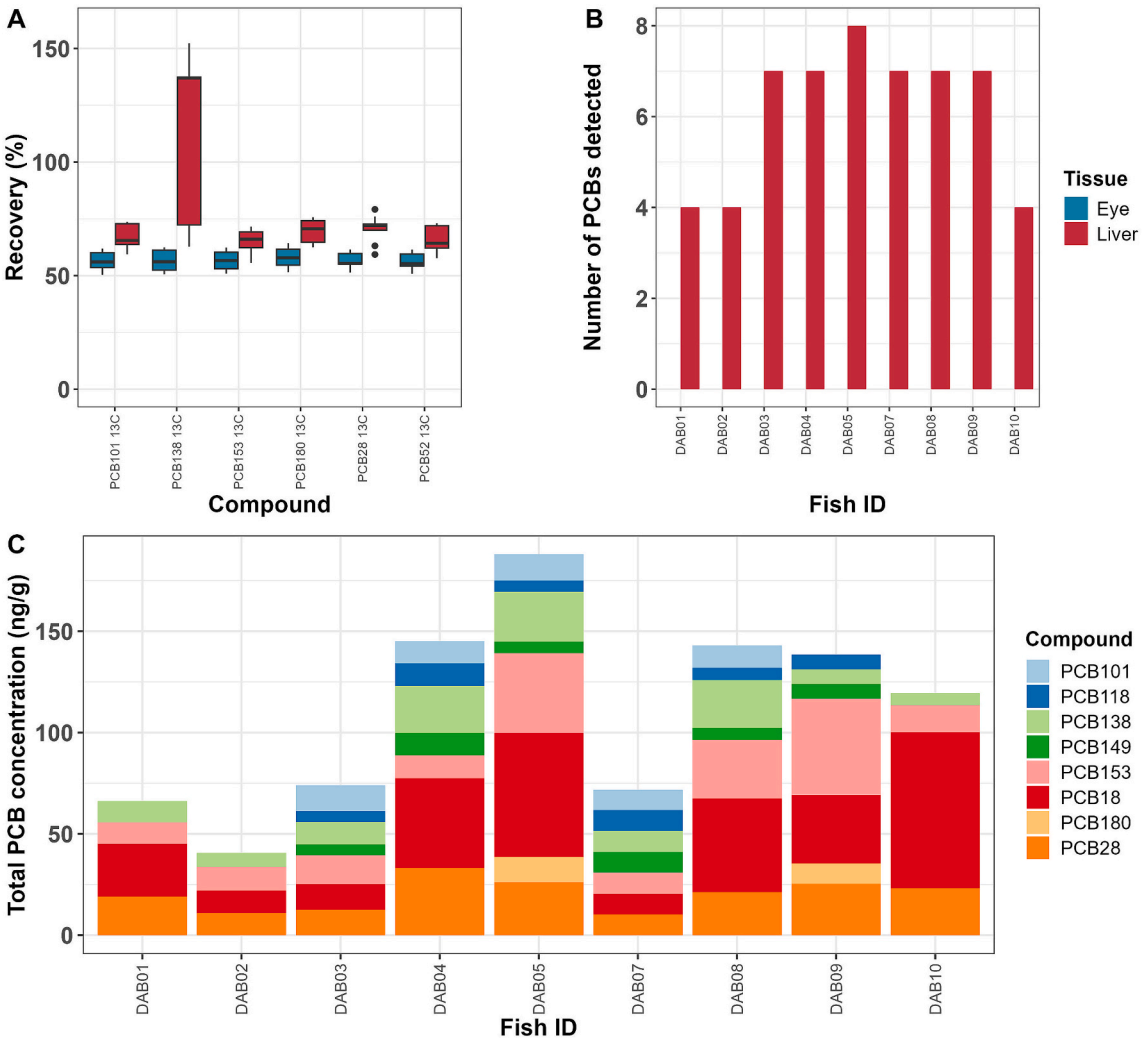

Fig. 7. SIM results for PCBs in dab liver subsamples and whole eye lenses. (A) Recovery rates for spike PCB internal standards in the two matrices. Boxes represent the interquartile range (IQR), with the centre line indicating the median. Whiskers extend to the most extreme value within 1.5 × IQR. (B) Number of PCBs detected in the 2 matrices showing no PCBs detected (>LOD) in any of the dab eye lenses. (C) Total PCB concentration in dab liver subsamples, coloured by PCB type.

Table 5
Gravimetric lipid content of eye lenses for dab and eels with the capsule on (first eye; as used for GCMS extraction) and capsule off (second eye). One lens from each of four individuals were pooled per sample.

			Capsule on (first eye)			Capsule off (second eye)		
Species	No. fish	Mean total length in cm (SD)	Combined eye lens weight (g)	Lipid weight (g)	% Lipid content	Combined eye lens weight (g)	Lipid weight (g)	% Lipid content
Dab	4	19.9 (0.6)	0.088882	0.00191	2.15%	0.083910	0.00226	2.69%
	4	21.6 (2.1)	0.098800	0.00190	1.92%	0.087906	0.00193	2.20%
	4	20.8 (1.6)	0.110492	0.00197	1.78%	0.097653	0.00130	1.33%
		Mean (SD)			1.95% (0.185%)			2.07% (0.689%)
Eel	4	37.35 (1.47)	0.031879	0.00155	4.86%			
	4	38.025 (1.26)	0.046294	0.00099	2.14%			
		Mean (SD)			3.50% (1.93%)			

narrower but higher-yield extraction of compounds of interest from eye lenses.

The recovery rates of internal standards were generally higher in eel eye lenses than the dab, potentially as a result of the higher lipid content of the eel lenses (1.79 times that of the dab lenses). This was expected as eels are generally more lipid-rich than many other fish species (Can Tunçelli, Özden and Erkan, 2022). Additionally, wide variation in the structure and hydration level of eye lenses within and between taxa has been previously documented (Quaeck-Davies et al., 2018) and so the bioconcentration rate of compounds in eye lenses will vary between species, as well as potentially the optimal sample preparation methods. For instance, elasmobranch lenses are more hydrated and less rigid than teleost lenses (Quaeck-Davies et al., 2018), while more rigid lenses may require more rigorous homogenisation techniques. Future studies may benefit from drying lenses first to aid with homogenisation and reduce variation in contaminant quantification caused by varying levels of

hydration. Further, lens porosity can vary between species (Quaeck-Davies et al., 2018) and the presence of aquaporins facilitating ion transport between laminae may enhance pollutant bioconcentration from the environment, but also increase susceptibility to laboratory contamination during sampling. While pollutants were expected to bind primarily to immobile protein fractions (crystallins), aquaporins may have also enabled their movement between laminae or the infiltration of contaminants during analysis. Despite differences in absolute recoveries, these were accounted for using internal standard recovery rates, and the method demonstrated consistent and reproducible performance within each species, supporting its utility for comparative exposure assessment and biomonitoring. To better assess cross-species applicability, future work would benefit from testing the method across a wider range of species while characterising lens physical properties.

The potential for lens porosity to increase risk of contamination also emphasises the need for process blanks in order to control for background contamination. Indeed, in the present study, numerous chemicals which can be used as plasticisers were detected in the untargeted screen. As every sample was blank-subtracted using a process blank, this is less likely to be an analytical artefact or result of laboratory-based contamination. However, the process blanks were not matrix-matched (i.e., they comprised only a spiked solvent), and so it is possible that laboratory-based contamination was not captured in the absences of e.g. lipids, in the same way that they were in the samples. The plasticisers indicated by the untargeted screen are worthy of future investigation but, due to the challenges of working with phthalic acid esters and other plasticisers (particularly the risk of background contamination), efforts were primarily focussed on PCBs, PAH and PAH derivatives instead. It is also important to note that the lenses in the present study included the capsule and were not rinsed before processing, and so the method cannot distinguish between recent, short term pollution exposure or lab contamination during handling captured on the outermost surfaces, vs. long term internal accumulation. Future studies should consider rinsing the lens in solvents prior to analysis. However, the lenses were dissected and minimally handled with the utmost care to avoid contamination, and given that the lens capsule only represents on average 4.51% (+/- 0.75% SD, n = 4 dab) of the full dry mass of the lens, it is unlikely that the contaminants observed were only present in or on the capsule.".

4.7. Future directions

We believe the key to improving the sensitivity of these methods lie in more targeted analysis. Where the present study began with untargeted screens with the aim to capture as many types of chemicals as possible due to no *a priori* assumptions on which may concentrate in lenses, future studies should focus on specific chemical classes. This will allow for more streamlined use of specialised extraction techniques, such as dichloromethane for the extraction of PAHs (Tsutsumi et al., 2021). More targeted and sensitive MS/MS methods, such as multiple reaction monitoring (MRM), which take full advantage of the triple quadrupole could also be employed depending on the chemical properties and stability of the target compounds. Although MRM is more selective and can achieve 10–25 fold lower LODs than SIM (Han et al., 2020), SIM analysis was used in the present study as PAHs are molecularly very stable and do not fragment readily in GC–MS (Moradi et al., 2020). PAH stability, combined with cost and ease of operation, has established SIM mode as the most popular method for PAH quantification in food and environmental samples (Poster et al., 2006). However, alternatives such as 'pseudo-MRM', which uses the molecular ion as both the precursor and product ion, can achieve 10–40 fold greater sensitivity compared with SIM across different molecular weights and may enable more selective PAH detection in future studies (Han et al., 2020; Galmiche et al., 2022).

Our data suggests that the low lipid content of lenses results in compound recoveries unaffected by chemical lipophilicity, and the main mechanism of uptake for organic pollutants in this tissue is via bioconcentration. This suggests the lens is more likely to favour moderately hydrophobic compounds, such as certain pesticides (e.g. atrazine (Huber, 1993)).

Controlled aquaria-based studies are a vital next step needed to validate our approach and progress this field of research towards real-world application. The exposure of fish to known concentrations of specific organic pollutants would elucidate uptake and toxicokinetic pathway(s), the timing of pollutant incorporation into the tissues, and validate the relationship between eye lens and ambient concentrations. Further, a controlled pulse exposure followed by a depuration period would be valuable to confirm the persistence of chemicals in the eye lens compared with soft tissues.

If future studies can achieve lamina −level resolution, this could be integrated with analysis of the otolith to infer age, and potentially location (depending on stable isotope analysis) to inform when and where exposure occurred. Such information would identify specific life-stages and habitats that are experiencing high pollution levels and need further protection or remediation efforts. The goal to understand historical conditions is gaining traction, and studies have now been able to use hormone profiles in opercula to reveal records of stress responses such as skipped spawning events or elevated cortisol (Charapata et al., 2022). The integration of such tools could elucidate the relationship between endpoints such as reduced growth or fecundity and pulse/historical exposure to sub-lethal chemical concentrations. Incorporating eye lens chemical assessments with isotopic chronologies to infer, for example, physiological conditions and trophic shifts, will also allow researchers to build a more comprehensive picture of the animal's exposome. A challenge facing the eco-exposome framework is the integration of an organism's cumulative lifetime exposure, particularly with regard to the timing of critical life stages (Scholz et al., 2022). Time-resolved historical chemical assessment would help to reconcile this and, even without chronological reconstruction, eye lenses could provide a more comprehensive lifetime chemical burden analysis by capturing historical chemical signals that may have been missed in soft tissue measurements due to tissue-specific differences in binding affinities, turnover rates, and their capacity to record intermittent exposure.

In summary, we have developed methods for the detection and quantification of organic pollutants in teleost eye lenses, although a robust level of sensitivity could not be achieved due to the low lipid content of lenses which impedes bioaccumulation rates. With further improvements to sensitivity, such as more targeted analysis and sample preparation, this system shows potential as a valuable tool for inferring pollution risk for key habitat and life stages, facilitating more targeted mitigation strategies.

CRediT authorship contribution statement

Rebekah Boreham: Writing – original draft, Visualization, Methodology, Investigation, Formal analysis. **Philip White:** Writing – review & editing, Methodology. **Boyd A. McKew:** Writing – review & editing, Methodology. **Sara Leston:** Writing – review & editing. **Andreia Freitas:** Writing – review & editing. **Jonathan L. Barber:** Writing – review & editing. **Michael Williamson:** Writing – review & editing. **Adam Piper:** Writing – review & editing. **Rosie Williams:** Writing – review & editing. **Anna M. Sturrock:** Writing – review & editing, Funding acquisition, Conceptualization.

Declaration of competing interest

The authors declare that they have no known competing financial interests or personal relationships that could have appeared to influence the work reported in this paper.

Acknowledgments

We would like to thank Clive Trueman (University of Southampton) for planting the idea in the first place; John Green (University of Essex) for performing the additional lab work for paper revisions and his assistance with maintenance and troubleshooting of the GC-MS/MS, and Erin Losty (Trinity College Dublin) for her help with the analysis software. Thank you also to Susanne Tanner (University of Lisbon), Vanessa Fonseca (University of Lisbon), and Deidre Brophy (Atlantic Technological University) for initial conversations and brainstorming. We also appreciate the conversations we had with John Bignell (Cefas) about this work and his help obtaining the dab. The collection of dab was funded by Defra through the Cefas Marine Systems Programme, which enhances the UK's ability to deliver scientific evidence and expert advice and provides access to unique marine science infrastructure. The programme supports data collection and scientific leadership across marine and freshwater environments, fisheries sustainability, international marine governance and marine incident response. The collection of eels was undertaken and funded by the Institute of Zoology. This study was funded by a UKRI Future Leaders Fellowship [MR/V023578/1].

Appendix A. Supplementary data

Supplementary data to this article can be found online at https://doi.org/10.1016/j.envint.2026.110400.

Data availability

Data will be made available on request.

References

Aerts, J. *et al.* (2015) 'Scales Tell a Story on the Stress History of Fish', *PLOS ONE*. Edited by D.E. Crocker, 10(4), p. e0123411. Doi: 10.1371/journal.pone.0123411.

Ajani Ek, K.O., Olanrewaju An, O.O., 2015. 'The sex ratio, gonadosomatic index, diet composition and fecundity of african pike, hepsetus odoe (Bloch, 1794) in Eleyele Lake, Nigeria'. Journal of Fisheries & Livestock Production 03 (03). https://doi.org/10.4172/2332-2608.1000139.

Alloy, M.M., et al., 2020. Exposure and recovery of the gulf toadfish (*Opsanus beta*) to weathered *deepwater horizon* slick oil: impacts on liver and blood endpoints. Environ. Toxicol. Chem. 40 (4), 1075–1086. https://doi.org/10.1002/etc.4966.

Barra, R.O., et al., 2021. Endocrine disruptor impacts on fish from chile: the influence of wastewaters. Front. Endocrinol. 12, 611281. https://doi.org/10.3389/fendo.2021.611281.

Barton, M.B., et al., 2019. Experimental determination of tissue turnover rates and trophic discrimination factors for stable carbon and nitrogen isotopes of Arctic Sculpin (Myoxocephalus scorpioides): a common Arctic nearshore fish. J. Exp. Mar. Biol. Ecol. 511, 60–67. https://doi.org/10.1016/j.jembe.2018.11.005.

Bassnett, S., Beebe, D.C., 1992. Coincident loss of mitochondria and nuclei during lens fiber cell differentiation. Dev. Dyn. 194 (2), 85–93. https://doi.org/10.1002/aja.1001940202.

Bell-Tilcock, M., et al., 2021. 'Advancing diet reconstruction in fish eye lenses'. Methods in Ecology and Evolution Edited by c. Trueman 12 (3), 449–457. https://doi.org/10.1111/2041-210X.13543.

Belpaire, C., et al., 2019. Impact of chemical pollution on Atlantic eels: facts, research needs, and implications for management. Curr. Opin. Environ. Sci. Health 11, 26–36. https://doi.org/10.1016/j.coesh.2019.06.008.

Benedetti, M., Giuliani, M.E., Regoli, F., 2015. Oxidative metabolism of chemical pollutants in marine organisms: molecular and biochemical biomarkers in environmental toxicology. Ann. N. Y. Acad. Sci. 1340 (1), 8–19. https://doi.org/10.1111/nyas.12698.

Bervoets, L., Blust, R., 2003. Metal concentrations in water, sediment and gudgeon (Gobio gobio) from a pollution gradient: relationship with fish condition factor. Environ. Pollut. 126 (1), 9–19. https://doi.org/10.1016/S0269-7491(03)00173-8.

Beyer, J., et al., 2010. Analytical methods for determining metabolites of polycyclic aromatic hydrocarbon (PAH) pollutants in fish bile: a review. Environ. Toxicol. Pharmacol. 30 (3), 224–244. https://doi.org/10.1016/j.etap.2010.08.004.

Bloemendal, H., et al., 2004. Ageing and vision: structure, stability and function of lens crystallins. Prog. Biophys. Mol. Biol. 86 (3), 407–485. https://doi.org/10.1016/j.pbiomolbio.2003.11.012.

Borchman, D., Yappert, M.C., 2010. Lipids and the ocular lens. J. Lipid Res. 51 (9), 2473–2488. https://doi.org/10.1194/jlr.R004119.

Bron, A.J., et al., 2000. The ageing lens. Ophthalmologica 214 (1), 86–104. https://doi.org/10.1159/000027475.

Can Tunçelli, İ., Özden, Ö., Erkan, N., 2022. Seasonal differences in lipid and fatty acid composition of european eels (anguilla anguilla, linnaeus 1758) from Orontes River, Turkiye. Aquatic Sciences and Engineering 37 (3), 169–174. https://doi.org/10.26650/ASE202221110462.

Charapata, P., et al., 2022. Lifetime hormone profiles for a long-lived teleost: opercula reveal novel estimates of age-specific reproductive parameters and stress trends in yelloweye rockfish (*Sebastes ruberrimus*). Can. J. Fish. Aquat. Sci. 79 (10), 1712–1728. https://doi.org/10.1139/cjfas-2022-0048.

Charapata, P., Horstmann, L. and Misarti, N. (2021) 'Steroid hormones in Pacific walrus bones collected over three millennia indicate physiological responses to changes in estimated population size and the environment', *Conservation Physiology*. Edited by S. Cooke, 9(1), p. coaa135. Doi: 10.1093/conphys/coaa135.

Chung, M.-T. *et al.* (2023) 'Species-specific trophic enrichment factor of stable nitrogen and carbon isotopes in fish otolith organic matter', *Marine and Freshwater Research*. Edited by I. Jones, 74(11), pp. 956–968. Doi: 10.1071/MF23022.

Diamante, G., et al., 2017. Developmental toxicity of hydroxylated chrysene metabolites in zebrafish embryos. Aquat. Toxicol. 189, 77–86. https://doi.org/10.1016/j.aquatox.2017.05.013.

Dolan, J., 2021. Chromatographic measurements, Part 5: determining LOD and LOQ based on the calibration curve. Separation Science [preprint].

Dove, S.G., Kingsford, M.J., 1998. Use of otoliths and eye lenses for measuring trace-metal incorporation in fishes: a biogeographic study. Mar. Biol. 130 (3), 377–387. https://doi.org/10.1007/s002270050258.

Du Plessis, A., 2019. *Water as an inescapable risk: current global water availability*. Quality and Risks with a Specific Focus on South Africa. Cham: Springer International Publishing (springer Water). https://doi.org/10.1007/978-3-030-03186-2.

EPA, 8270 E (2018) *EPA Method 8270, Semivolatile Organic Compounds by GC/MS*. U.S. EPA Test Methods 64. Available at: https://www.epa.gov/sites/default/files/2020-10/documents/method_8270e_update_vi_06-2018_0.pdf.

Fernandez-Lopez, L., et al., 2019. Development and validation of a gas chromatography–mass spectrometry method for opiates and cocaine in human bone. J. Pharm. Biomed. Anal. 164, 636–641. https://doi.org/10.1016/j.jpba.2018.11.015.

Fey, S.B., et al., 2015. Recent shifts in the occurrence, cause, and magnitude of animal mass mortality events. Proc. Natl. Acad. Sci. 112 (4), 1083–1088. https://doi.org/10.1073/pnas.1414894112.

Frapiccini, E., et al., 2018. Polycyclic aromatic hydrocarbon (PAH) accumulation in different common sole (Solea solea) tissues from the North Adriatic Sea peculiar impacted area. Mar. Pollut. Bull. 137, 61–68. https://doi.org/10.1016/j.marpolbul.2018.10.002.

Galmiche, M., et al., 2022. The use of pseudo-MRM for a sensitive and selective detection and quantification of polycyclic aromatic compounds by tandem mass spectrometry. Rapid Commun. Mass Spectrom. 36 (13), e9307.

Golikov, A.V., et al., 2024. Insights on long-term ecosystem changes from stable isotopes in historical squid beaks. BMC Ecol. Evol. 24 (1), 90. https://doi.org/10.1186/s12862-024-02274-7.

Hamilton, P.B., et al., 2016. Population-level consequences for wild fish exposed to sublethal concentrations of chemicals – a critical review. Fish Fish. 17 (3), 545–566. https://doi.org/10.1111/faf.12125.

Han, Y., et al., 2020. Understanding the relative performance of SCAN, SIM, PMRM and MRM methods for quantifying polycyclic aromatic hydrocarbons in crude oil samples. Rapid Commun. Mass Spectrom. 34 (11), e8765.

Hauser-Davis, R.A., et al., 2021. Perfluoroalkyl substances associations with morphometric health indices in three fish species from differentially contaminated water bodies in Southeastern Brazil. Environ. Technol. Innovation 21, 101198. https://doi.org/10.1016/j.eti.2020.101198.

Honda, M., Suzuki, N., 2020. Toxicities of polycyclic aromatic hydrocarbons for aquatic animals. Int. J. Environ. Res. Public Health 17 (4), 1363. https://doi.org/10.3390/ijerph17041363.

Huber, W., 1993. Ecotoxicological relevance of atrazine in aquatic systems. Environ. Toxicol. Chem. 12 (10), 1865–1881. https://doi.org/10.1002/etc.5620121014.

IUCN (2013) 'Anguilla anguilla: Jacoby, D. & Gollock, M.: The IUCN Red List of Threatened Species 2014: e.T60344A45833138'. Doi: 10.2305/IUCN.UK.2014-1.RLTS.T60344A45833138.en.

Jacoby, D.M.P., et al., 2015. Synergistic patterns of threat and the challenges facing global anguillid eel conservation. Global Ecol. Conserv. 4, 321–333. https://doi.org/10.1016/j.gecco.2015.07.009.

Jacquin, L., et al., 2020. Effects of pollution on fish behavior, personality, and cognition: some research perspectives. Front. Ecol. Evol. 8, 86. https://doi.org/10.3389/fevo.2020.00086.

James, M.O., Kleinow, K.M., 2014. Seasonal influences on PCB retention and biotransformation in fish. Environ. Sci. Pollut. Res. 21 (10), 6324–6333. https://doi.org/10.1007/s11356-013-1611-3.

Johnson, R.C., et al., 2020. Lifetime chronicles of selenium exposure linked to deformities in an imperiled migratory fish. Environ. Sci. Technol. 54 (5), 2892–2901. https://doi.org/10.1021/acs.est.9b06419.

Khorshid, M., et al., 2015. QuEChERS method followed by solid phase extraction method for gas chromatographic-mass spectrometric determination of polycyclic aromatic hydrocarbons in fish. International Journal of Analytical Chemistry 2015, 1–7. https://doi.org/10.1155/2015/352610.

Kiss, A.J., Devries, A.L., Morgan-Kiss, R.M., 2010. Comparative analysis of crystallins and lipids from the lens of Antarctic toothfish and cow. J. Comp. Physiol. B 180 (7), 1019–1032. https://doi.org/10.1007/s00360-010-0475-9.

Kuntz, J.P. *et al.* (2024) 'Investigating eye lens composition for stable isotope analysis in fishes: a comparison between Chondrichthyes and Actinopterygii', *Environmental Biology of Fishes* [Preprint]. Doi: 10.1007/s10641-024-01656-6.

Lawal, A.T. (2017) 'Polycyclic aromatic hydrocarbons. A review', *Cogent Environmental Science*. Edited by P. Fantke, 3(1), p. 1339841. Doi: 10.1080/23311843.2017.1339841.

Liang, Y., et al., 2007. Distribution patterns of polycyclic aromatic hydrocarbons (PAHs) in the sediments and fish at Mai Po Marshes Nature Reserve, Hong Kong. Water Res. 41 (6), 1303–1311. https://doi.org/10.1016/j.watres.2006.11.048.

Limburg, K.E., et al., 2015. In search of the dead zone: use of otoliths for tracking fish exposure to hypoxia. J. Mar. Syst. 141, 167–178. https://doi.org/10.1016/j.jmarsys.2014.02.014.

Lynnerup, N. *et al.* (2008) 'Radiocarbon Dating of the Human Eye Lens Crystallines Reveal Proteins without Carbon Turnover throughout Life', *PLoS ONE*. Edited by E. Gazit, 3(1), p. e1529. Doi: 10.1371/journal.pone.0001529.

Madigan, D.J. *et al.* (2012) 'Tissue Turnover Rates and Isotopic Trophic Discrimination Factors in the Endothermic Teleost, Pacific Bluefin Tuna (Thunnus orientalis)', *PLoS ONE*. Edited by J.V. Planas, 7(11), p. e49220. Doi: 10.1371/journal.pone.0049220.

Malaj, E., et al., 2014. Organic chemicals jeopardize the health of freshwater ecosystems on the continental scale. Proc. Natl. Acad. Sci. 111 (26), 9549–9554. https://doi.org/10.1073/pnas.1321082111.

Mali, M., et al., 2022. Improved identification of pollution source attribution by using PAH ratios combined with multivariate statistics. Sci. Rep. 12 (1), 19298. https://doi.org/10.1038/s41598-022-23966-4.

Miraly, H., et al., 2023. Tracking fish lifetime exposure to mercury using eye lenses. Environ. Sci. Technol. Lett. 10 (3), 222–227. https://doi.org/10.1021/acs.estlett.2c00755.

Moradi, V., et al., 2020. Development of a GC-MS method for determination of various polycyclic aromatic hydrocarbons in iranian traditional and semi-industrial taftoon bread. Iranian Journal of Pharmaceutical Research 19 (3). https://doi.org/10.22037/ijpr.2019.15323.13018.

Morado, C.N., Araújo, F.G., Gomes, I.D., 2017. <**b>The use of biomarkers for assessing effects of pollutant stress on fish species from a tropical river in Southeastern Brazil. Acta Scientiarum. Biological Sciences 39 (4), 431. https://doi.org/10.4025/actascibiolsci.v39i4.34293.

Mustafa, S.A., Al-Rudainy, A.J., Salman, N.M., 2024. Effect of environmental pollutants on fish health: an overview. Egypt. J. Aquat. Res. 50 (2), 225–233. https://doi.org/10.1016/j.ejar.2024.02.006.

Neff, J.M., Stout, S.A., Gunster, D.G., 2005. Ecological risk assessment of polycyclic aromatic hydrocarbons in sediments: Identifying sources and ecological hazard. Integr. Environ. Assess. Manag. 1 (1), 22–33. https://doi.org/10.1897/IEAM_2004a-016.1.

Neis, B., et al., 2023. Mass mortality events in marine salmon aquaculture and their influence on occupational health and safety hazards and risk of injury. Aquaculture 566, 739225. https://doi.org/10.1016/j.aquaculture.2022.739225.

Olivares-Rubio, H.F., Arce, E., 2023. Effects of chemical pollution on the behaviour of cichlid fish. Environ. Biol. Fishes 106 (5), 1149–1176. https://doi.org/10.1007/s10641-022-01376-9.

Pal, A., et al., 2010. Impacts of emerging organic contaminants on freshwater resources: review of recent occurrences, sources, fate and effects. Sci. Total Environ. 408 (24), 6062–6069. https://doi.org/10.1016/j.scitotenv.2010.09.026.

Parzanini, C., et al., 2021. Feeding habitat and silvering stage affect lipid content and fatty acid composition of European eel Anguilla anguilla tissues. J. Fish Biol. 99 (3), 1110–1124. https://doi.org/10.1111/jfb.14815.

Peebles, E.B., Hollander, D.J., 2020. Combining isoscapes with tissue-specific isotope records to recreate the geographic histories of fish. In: Murawski, S.A. (Ed.), *Scenarios and Responses to Future Deep Oil Spills*. Springer International Publishing, Cham, pp. 203–218. https://doi.org/10.1007/978-3-030-12963-7_12.

Pinkney, A.E., et al., 2001. Tumor prevalence and biomarkers of exposure in brown bullheads (*Ameiurus nebulosus*) from the tidal Potomac River, USA, watershed. Environ. Toxicol. Chem. 20 (6), 1196–1205. https://doi.org/10.1002/etc.5620200608.

Poster, D.L., et al., 2006. Analysis of polycyclic aromatic hydrocarbons (PAHs) in environmental samples: a critical review of gas chromatographic (GC) methods. Anal. Bioanal. Chem. 386 (4), 859–881. https://doi.org/10.1007/s00216-006-0771-0.

Pulster, E.L., et al., 2017. Species-specific metabolism of naphthalene and phenanthrene in 3 species of marine teleosts exposed to *Deepwater Horizon* crude oil. Environ. Toxicol. Chem. 36 (11), 3168–3176. https://doi.org/10.1002/etc.3898.

Qin, N., et al., 2020. 'Tissue distribution, bioaccumulation, and carcinogenic risk of polycyclic aromatic hydrocarbons in aquatic organisms from Lake Chaohu, China'. Sci. Total Environ. 749, 141577. https://doi.org/10.1016/j.scitotenv.2020.141577.

Quaeck-Davies, K., et al., 2018. Teleost and elasmobranch eye lenses as a target for life-history stable isotope analyses. PeerJ 6, e4883.

R Core Team (2023) '_R: A Language and Environment for Statistical Computing_.' Vienna, Austria: R Foundation for Statistical Computing. Available at: https://www.R-project.org/.

Rahmanpour, S., Farzaneh Ghorghani, N., Lotfi Ashtiyani, S.M., 2014. Polycyclic aromatic hydrocarbon (PAH) in four fish species from different trophic levels in the Persian Gulf. Environ. Monit. Assess. 186 (11), 7047–7053. https://doi.org/10.1007/s10661-014-3909-0.

Reis-Santos, P., et al., 2023. Reading the biomineralized book of life: expanding otolith biogeochemical research and applications for fisheries and ecosystem-based management. Rev. Fish Biol. Fish. 33 (2), 411–449. https://doi.org/10.1007/s11160-022-09720-z.

Rijnsdorp, A.D., et al., 1992. Recruitment of sole stocks, Solea solea (L.), in the Northeast Atlantic. Neth. J. Sea Res. 29 (1–3), 173–192. https://doi.org/10.1016/0077-7579(92)90018-A.

Sakamoto, T., et al., 2017. Temperature dependence of δ 18 O in otolith of juvenile Japanese sardine: laboratory rearing experiment with micro-scale analysis. Fish. Res. 194, 55–59. https://doi.org/10.1016/j.fishres.2017.05.004.

Sakamoto, T., et al., 2023. 'Stable isotopes in eye lenses reveal migration and mixing patterns of diamond squid in the western North Pacific and its marginal seas'. ICES Journal of Marine Science Edited by a. Andrews 80 (9), 2313–2328. https://doi.org/10.1093/icesjms/fsad145.

Scholz, S., et al., 2022. The eco-exposome concept: supporting an integrated assessment of mixtures of environmental chemicals. Environ. Toxicol. Chem. 41 (1), 30–45. https://doi.org/10.1002/etc.5242.

Sturrock, A.M., et al., 2015. 'Quantifying physiological influences on otolith microchemistry'. Methods in Ecology and Evolution. Edited by e. Leder 6 (7), 806–816. https://doi.org/10.1111/2041-210X.12381.

Tobiszewski, M., Namieśnik, J., 2012. PAH diagnostic ratios for the identification of pollution emission sources. Environ. Pollut. 162, 110–119. https://doi.org/10.1016/j.envpol.2011.10.025.

Topić Popović, N., et al., 2023. Fish liver damage related to the wastewater treatment plant effluents. Environ. Sci. Pollut. Res. 30 (17), 48739–48768. https://doi.org/10.1007/s11356-023-26187-y.

Tsutsumi, T., et al., 2021. A novel analytical method for determining total polychlorinated biphenyl concentrations in fish and shellfish using a simple and rapid clean-up followed by GC–MS/MS. J. Food Compos. Anal. 96, 103725. https://doi.org/10.1016/j.jfca.2020.103725.

Tzadik, O.E., et al., 2017. Chemical archives in fishes beyond otoliths: a review on the use of other body parts as chronological recorders of microchemical constituents for expanding interpretations of environmental, ecological, and life-history changes. Limnol. Oceanogr. Methods 15 (3), 238–263. https://doi.org/10.1002/lom3.10153.

Van Der Oost, R., et al., 1994. Biochemical markers in feral roach (Rutilus rutilus) in relation to the bioaccumulation of organic trace pollutants. Chemosphere 29 (4), 801–817. https://doi.org/10.1016/0045-6535(94)90048-5.

Van Der Oost, R., Beyer, J., Vermeulen, N.P.E., 2003. Fish bioaccumulation and biomarkers in environmental risk assessment: a review. Environ. Toxicol. Pharmacol. 13 (2), 57–149. https://doi.org/10.1016/S1382-6689(02)00126-6.

Volk, E.C., et al., 2000. Otolith chemistry reflects migratory characteristics of Pacific salmonids. Fish. Res. 46 (1–3), 251–266. https://doi.org/10.1016/S0165-7836(00)00150-8.

Wallace, A.A., Hollander, D.J. and Peebles, E.B. (2014) 'Stable Isotopes in Fish Eye Lenses as Potential Recorders of Trophic and Geographic History', *PLoS ONE*. Edited by A. Chiaradia, 9(10), p. e108935. Doi: 10.1371/journal.pone.0108935.

Wang, D., et al., 2022. Increasingly frequent extreme weather events urge the development of point-of-use water treatment systems. npj Clean Water 5 (1), 36. https://doi.org/10.1038/s41545-022-00182-1.

Wang, S., et al., 2024. Assessing the ecological impacts of polycyclic aromatic hydrocarbons petroleum pollutants using a network toxicity model. Environ. Res. 245, 117901. https://doi.org/10.1016/j.envres.2023.117901.

Whelan, M.J., et al., 2022. Is water quality in british rivers "better than at any time since the end of the Industrial Revolution"? Sci. Total Environ. 843, 157014. https://doi.org/10.1016/j.scitotenv.2022.157014.

Young, M.J., et al., 2022. Eye lenses reveal ontogenetic trophic and habitat shifts in an imperiled fish, Clear Lake hitch (*Lavinia exilicauda chi*). Can. J. Fish. Aquat. Sci. 79 (1), 21–30. https://doi.org/10.1139/cjfas-2020-0318.